



Performance modeling of Deep Burn TRISO fuel using ZrC as a load-bearing layer and an oxygen getter

Doonyapong Wongsawaeng*

Nuclear Technology Department, Faculty of Engineering, Chulalongkorn University, Bangkok 10330, Thailand
General Atomics Company, San Diego, CA 92121, USA

ARTICLE INFO

Article history:

Received 3 August 2007

Accepted 28 October 2009

ABSTRACT

The effects of design choices for the TRISO particle fuel were explored in order to determine their contribution to attaining high-burnup in Deep Burn modular helium reactor fuels containing transuranics from light water reactor spent fuel. The new design features were: (1) ZrC coating substituted for the SiC, allowing the fuel to survive higher accident temperatures; (2) pyrocarbon/SiC “alloy” substituted for the inner pyrocarbon coating to reduce layer failure and (3) pyrocarbon seal coat and thin ZrC oxygen getter coating on the kernel to eliminate CO. Fuel performance was evaluated using General Atomics Company’s PISA code. The only acceptable design has a 200- μm kernel diameter coupled with at least 150- μm thick, 50% porosity buffer, a 15- μm ZrC getter over a 10- μm pyrocarbon seal coat on the kernel, an alloy inner pyrocarbon, and ZrC substituted for SiC. The code predicted that during a 1600 °C postulated accident at 70% FIMA, the ZrC failure probability is $<10^{-4}$.

© 2009 Elsevier B.V. All rights reserved.

1. Introduction

The Deep Burn reactor proposed by the General Atomics Company [1] utilizes reprocessed spent nuclear fuel from light water reactors. Recovered plutonium (mostly ^{239}Pu) and other minor transuranics are fabricated into TRISO fuel particles. ^{238}U , which typically accounts for at least 95% of the spent fuel mass, and a miniscule amount of ^{235}U and ^{236}U separated from the spent fuel are to be reused in LWRs. For a one-pass Deep Burn cycle in a 600 MW_t Gas-Turbine Modular Helium Reactor (GT-MHR) operating at 1000 °C, the transuranic materials are irradiated to a very high maximum burnup of 70% FIMA (fission per initial metal atom). The spent fuel is sent directly to the repository. This exceptionally high-burnup is achievable because of the special properties of the coated particle fuel employing ZrC.

Deep Burn meets the three objectives of the nuclear industry and the new GNEP initiative: (1) efficient utilization of energy in spent fuel; (2) reduction in waste volume and (3) proliferation resistance (essentially no fissile material in the fuel sent to the repository).

The current design of SiC-coated TRISO fuel particles used in GT-MHR has a spherical oxide kernel containing fissile materials. The kernel is fabricated by a sol-gel technique. A typical size of the fissile kernel is 200–500 μm in diameter. A CVD-deposited buffer

layer (50% dense pyrolytic carbon) surrounding the kernel provides free space for fission gases and for kernel expansion due to solid fission product swelling and fission gas bubble formation. Fission recoils are stopped in the layer. The buffer condenses during the course of irradiation. A typical buffer thickness is 100 μm . An inner pyrocarbon layer (IPyC) is CVD-deposited on top of the buffer layer. Although this layer confines fission gases, most of solid fission products can easily diffuse through it. Due to the crystal structure of pyrolytic carbon, it shrinks under fast neutron irradiation. The magnitudes of the shrinkages on the tangential and radial directions depend on the layer isotropy, density, temperature, and fast neutron fluence. The PyC shrinkage in the tangential direction (which is parallel to the SiC deposition plane) places a compressive load on the SiC while the counteracting effect of fission-gas pressure adds a tensile stress to it. A typical IPyC thickness is 35 μm . An intact high density IPyC also protects the kernel from chlorine attack, as chlorine-bearing gas is used to deposit SiC.

A dense, CVD-deposited ceramic SiC layer on top of the IPyC functions as a main load-bearing layer and as a fission product containment. An intact SiC coat retains both gaseous and metallic fission products except $^{110\text{m}}\text{Ag}$, which can pass through at temperatures above 1000 °C. A typical SiC thickness is 35 μm . The outermost layer is a CVD-deposited outer pyrolytic carbon (OPyC). Its main role is to isolate SiC from the surroundings, and when it shrinks, it compresses the SiC layer.

To fabricate a fuel compact, fuel particles are mixed together with a graphite binder, formed into a cylinder 12.7 mm in diameter and 50.8 mm long. Then, it is fired at high temperature to carbonize

* Address: Nuclear Technology Department, Faculty of Engineering, Chulalongkorn University, Phayathai Road, Phatumwan, Bangkok 10330, Thailand. Tel.: +66 080 441 4509; fax: +66 02 218 6780.

E-mail address: Doonyapong.W@Chula.ac.th

Table 1
Elemental composition of the Deep Burn kernel (oxides).

Element	Atom (%)
Pu	85
Np	5
Am	9
Cm	1

the binder. Failure of SiC during compact manufacturing due to particle-to-particle contact is reduced significantly by pre-applying an over-coating layer – another layer of the graphite binder – to the particles.

2. Evaluating the new design features

Each of the new design features was evaluated using a fuel performance code. Evaluations were made on:

- Conventional TRISO.
- ZrC substituted for SiC (ZrC-coated TRISO).
- ZrC getter on kernel with
 - o Conventional TRISO.
 - o ZrC-coated TRISO.
- Alloy IPyC with
 - o Normal TRISO.
 - o ZrC-coated TRISO.
 - o Conventional TRISO with ZrC getter on kernel.
 - o ZrC-coated TRISO with ZrC getter on kernel.

For all cases, a steady-state temperature of 1000 °C¹ from the BOL to the maximum EOL burnup of 70% FIMA, reaching a fast fluence of 4×10^{25} n/m², was assumed. A postulated accident scenario causing the fuel temperature to reach 1600 °C three days after the EOL burnup was assumed. A constant temperature gradient of 10⁴ K/m across the fuel particle² was used during the irradiation period. Material properties of the particle fuel were assumed unchanged with fast neutron fluence, include during the accident. To allow comparison of all the cases on the same basis, a kernel diameter of 200 μm, a buffer thickness of 100 μm, an IPyC (or alloy PyC) thickness of 35 μm, an SiC (or ZrC) thickness of 35 μm, and an OPyC thickness of 40 μm were assumed. A PyC seal coat thickness of 10 μm and a ZrC getter thickness of 15 μm³ were assumed for designs employing the ZrC scavenger. Fabrication defect of SiC (and ZrC) was taken to be 10⁻⁵.

Literature search revealed the volumetric kernel swelling due to solid fission products to be as low as 0.35% [2] and as high as 1% [3] per % FIMA. Although the values were for UO₂, they were assumed to apply to the Deep Burn kernel composing mostly of plutonium oxide. For conservative estimates, the volumetric swelling of 1% per % FIMA was adopted. Kernel swelling increased fission-gas pressure because of the reduction in the in-particle free volume.

3. In-particle gas pressure

3.1. Fission-gas pressure

Fission-gas pressure as function of burnup and temperature was calculated and manually input. The total yield of Xe and Kr was

¹ A typical average fuel temperature. Although peak fuel temperatures for VHTRs are typically 1200–1250 °C, it will be shown later that the kernel size, the buffer thickness and the ZrC getter, not the steady-state temperature, are the main parameters in determining the fuel failure during the postulated EOL accident.

² A typical value based on General Atomics Company's literature.

³ The thickness of ZrC required to consume all of the oxygen anticipated released from fission up to the EOL burnup is only a few microns. The proposed PyC seal coat and ZrC getter thicknesses accommodate fabrication, since a coating layer of only a few microns thick would not be practical to fabricate reliably.

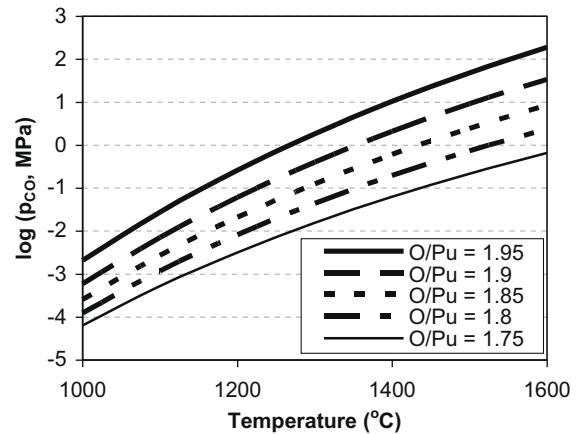


Fig. 1. Predicted CO pressure under different temperatures and O/Pu ratios.

27.2%, calculated by weighting the yields from ²³⁹Pu and ²⁴¹Am obtained from Ref. [4] by their corresponding atomic fractions in the kernel shown in Table 1.

All fission gas atoms were assumed to leave the kernel and stay in the buffer porosity, for conservative estimates. This is not the case in reality, however, as micro and macro fission-gas bubbles of various sizes form in the kernel, and as a portion of the gas atoms remains atomically dispersed in the kernel matrix. For the purpose of calculating fission-gas pressure, the buffer was taken to be 50% dense and remained 50% dense through the end of accident. Although buffer densification does occur, the total free space in the buffer layer (less that taken up by the swollen kernel) should not change substantially.

3.2. CO pressure

Following the worst-case scenario for Deep Burn, a 1600 °C accident at 70% FIMA, the carbon monoxide pressure⁴ would be very large. The effect of temperature and O/Pu ratio on the CO pressure was studied and is demonstrated in Fig. 1. The required governing equation for the oxygen potential of PuO_{2-x}⁵ as a function of oxygen stoichiometry and temperature was adopted from Lindemer's work [4]. The standard-state Gibb's formation energy of the O₂ + 2C ⇌ 2CO reaction required to establish the CO pressure was obtained from Ref. [4]. Note that the CO pressure is thermodynamically-controlled. It does not depend on the in-particle free volume. At 70% FIMA and 1600 °C, the O/Pu ratio becomes very high, most likely reaching at least 1.92,⁶ corresponding to a CO pressure in excess of 60 MPa. Fission-gas pressure calculated in the preceding section augments the CO pressure by a minimum of tens of MPa, depending on the kernel size and buffer thickness, making the overall internal gas pressure close to 100 MPa.

3.3. Americium pressure

Americium vaporization from metallic and oxide systems was investigated by Lindemer [4]. According to the Ellingham diagram of the Am–O–C system [4], at 1600 °C, Am gas contributes the largest partial pressure among the Am-containing gaseous species (Am, AmO, and AmO₂). However, at 1600 °C, the pressure is always

⁴ Fissioning of uranium or plutonium oxide liberates oxygen atoms. A portion of them combines with fission products to form stable fission product oxides. The remaining unbound oxygen diffuses out of the kernel and combines with carbon in the buffer layer to form the CO gas.

⁵ PuO_{2-x} is a conventional short-hand notation for a mixture of PuO₂ and Pu₂O₃. For example, PuO_{1.68} represents a mixture of 0.36 mol of PuO₂ and 0.32 mol of Pu₂O₃.

⁶ From interpolation of entries in Table 6 of Ref. [4].

Table 2
Input values for material properties.

Properties	IPyC and OPyC [8]	ZrC	SiC [8]
Young's modulus (MPa)	3.30×10^4	4×10^5 [9]	3.7×10^5
Poisson's ratio	0.23	0.25 [10]	0.13
Creep Poisson's ratio	0.4	n/a	n/a
Thermal expansion coefficient (K^{-1})	5.57×10^{-6}	7.1×10^{-6} [9,11,12]	4.9×10^{-6}
σ_0 (MPa $\times m^{3/m}$)	18.53	6.75, 4.82, 2.89, 0.964	9.64
m	9.5	6	6
Creep coefficient (MPa $^{-1}$), from Eqs. (2) and (3)	2.21×10^{-4} at 1000 °C, 7.67×10^{-4} at 1600 °C	n/a	n/a
BAF (anisotropy factor)	1.036	n/a	n/a

less than 10 kPa under any oxygen potential. An Americium pressure of 0.1 MPa would be established at ~ 2050 °C under an oxygen potential of less than -780 kJ/mol. Thus, Am vaporization poses no risk to substantially increase the in-particle pressure. Americium loss by this mechanism, however, could be problematic during kernel fabrication if the temperature and the oxygen potential are not properly controlled.

4. General Atomics' particle fuel performance code

General Atomics' proprietary PC-based code named PISA (Particle Irradiation Stress Analysis) is a one-dimensional finite-element code used to analyze stresses in the particle layers [5]. The code was written in C++ and incorporated several phenomena necessary for accurate performance predictions, which included irradiation-induced dimensional changes for PyC materials, irradiation-assisted creep strain for PyC materials, linear elastic and linear viscoelastic (for PyC) material models, thermal stress and strain, and stresses due to pressure.

Prediction of the failure probability of each layer employs a Weibull method. This well-known technique applies to brittle materials, as it predicts stress-induced failure by assuming the presence of defects of various sizes in the structure according to the Weibull distribution:

$$p = 1 - \exp\left(-\int_V (\sigma_{\max}/\sigma_0)^m dV\right), \quad (1)$$

where p is the failure probability of the layer; σ_{\max} , the maximum stress in the layer; σ_0 , the Weibull characteristic strength of the material, obtained from a three-point bend test; m , the Weibull modulus of the material, obtained from a three-point bend test and V is the volume of the layer.

PISA takes into account degradation of SiC due to fission product reactions and coating failure due to kernel migration⁷, both using models in Ref. [6]. The SiC-fission product corrosion mechanism applies up to 1600 °C, above which SiC thermal decomposition is believed to be the main mode of SiC failure. Kernel migration takes place only during normal operations when there exists a temperature gradient across the particle. However, the code does not account for the stress intensity factor at the tip of a crack in the IPyC (or the OPyC), which could result in a premature SiC failure. The code does not model other failure mechanisms such as debonding of the IPyC from the SiC, and potential rigid contact between the kernel and the IPyC. The code cannot account for the effect of particle asphericity as it solves problems in a one-dimensional space.

Stress and failure predictions by PISA exhibited good agreements with several other codes whose authors participated in an IAEA's Coordinated Research Program on coated particle fuel technology under normal operating conditions [7].

⁷ Under normal operating conditions, probability of coating failure due to kernel migration is $\ll 10^{-6}$.

5. Material properties of coating layer

Table 2 lists material properties that PISA requires.

An original form of the equation to calculate creep coefficient for pyrocarbon materials was adopted from General Atomics [8]. As suggested in Ref. [13] that the pyrocarbon creep be multiplied by 1.8 to better match experimental data, the final form of the equation became:

$$K_s = 1.8 \times K_{so}[1 + (1.9 - \rho) \times 2.38], \quad (2)$$

$$K_{so} = 2.193 \times 10^{-4} - 4.85 \times 10^{-7}(T + 273) + 4.0147 \times 10^{-10}(T + 273)^2, \quad (3)$$

where K_s is the creep coefficient (1/MPa); K_{so} , the value of K_s at $\rho = 1.9$ g/cm³; ρ , the pyrocarbon density, ≈ 1.94 g/cm³ and T is the temperature (°C).

Material properties for the kernel and buffer were not listed in Table 2 because they were not modeled by PISA. They have no direct mechanical effect on stresses in the IPyC, SiC (or ZrC), and OPyC. The only direct effect is the gas pressure acting on the inner wall of the IPyC, which depends on the buffer porosity, buffer thickness, kernel composition, kernel size, temperature and burnup.

6. Evaluating conventional TRISO

Performance of conventional SiC-coated TRISO with no oxygen getter and an IPyC alloy was evaluated. Since the CO pressure during the postulated EOL accident could not be estimated with high accuracy because the exact oxygen stoichiometry in PuO_{2-x} was not known, values of 60 MPa and 100 MPa were assumed. During the accident, the SiC failure was predicted to be:

- $10^{-2.11}$ for the case with 100 MPa of CO pressure, and
- $10^{-3.07}$ for the case with 60 MPa of CO pressure.

These very high failures were due to the large CO pressure. Obviously, an oxygen getter to suppress CO formation would be needed. Fig. 5 summarizes predictions of SiC (or ZrC) failure for all cases.

7. Evaluating ZrC as a substitute for SiC

At high temperatures, SiC is susceptible to fission product corrosion especially by Pd (via a Pd₂Si intermetallic formation [14]), the lanthanide series and metallic inclusions in the fuel notably iron. It also thermally decomposes significantly starting at ~ 1700 °C by transformation from β -SiC to α -SiC [15], resulting in a loss of integrity.

7.1. Advantages

7.1.1. Higher melting/decomposition temperature

Zirconium carbide is a refractory and chemically stable compound. The melting point is 3540 °C and it melts eutectically with

Table 3
Test conditions of ZrC-coated particle fuel and results.

Ref.	Irradiation condition			Post-irradiation condition		Results
	Temperature (°C)	FIMA (%)	EFPD	Temperature (°C)	Time (h)	
[17]	1400–1650	4.5	99.9	–	–	Zero or 1 particle, at most, in 2400 particles experienced through-wall failure. No palladium attack or thermal decomposition. SiC-coated particles irradiated concurrently exhibited ~20 particles with through-wall failure
[18]	900	1.5	79.9	1600	4500	No pressure vessel failure during heating test, no palladium attack, or thermal decomposition. High ¹³⁷ Cs retention
[19]	900	1.5	79.9	1800–2000	3000 and 100	No through-wall failure and high ¹³⁷ Cs retention up to 1800 °C (only release behavior of fission products was studied)
[20]	1100	4	81.2	2400	1.67	No particle failure until one failed among 101 particles after 6000 s. Concluded that at 2400 °C, SiC was brittle while ZrC could sustain a very large strain

carbon at 2850 °C [16]. It maintains excellent thermal stability at 1600 °C [14].

7.1.2. Less susceptibility to fission product attack

ZrC is less susceptible to palladium [14] and other noble metallic fission product attack than SiC [4]. The layer integrity is thus maintained much better than SiC. However, according to Ref. [14], reaction of Pd with ZrC occurs only when the Pd concentration becomes large. Furthermore, Ref. [17] points out that while there was no observable ZrC attack by palladium, it may be because Pd diffused through the layer and never reached the critical concentration. In fact, an electron probe micro analysis (EPMA) of irradiated fuel at 1400–1650 °C revealed no Pd attack or accumulation of Pd at the inner wall of ZrC [17]. More irradiation and heating tests are needed to better understand this important issue because at 70% burnup, the Pd inventory in the kernel and surrounding the particle fuel may far surpass the minimum concentration required to initiate the Pd–ZrC reaction.

7.1.3. Excellent performance in low burnup irradiation and heating tests

Several low-burnup short-duration irradiation and post-irradiation heating tests have been performed on UO₂ ZrC TRISO-coated fuel particles. Table 3 summarizes the test conditions and outcomes.

According to the irradiation results discussed in Ref. [20], although ~1% of particles failed shortly after ~1.7 h into the heating test, the heating temperature of 2400 °C was much higher than anticipated during a postulated GT-MHR transient accident. Conventional SiC-coated particles, if heated to 2400 °C, would experience failure of ~20%–90% according to General Atomics' prediction [21]. Therefore, if fuel particles would ever reach this very high accident temperature, ZrC would still exhibit a superior fission product retention capability than SiC.

7.1.4. Retention of fission products

Silver is not effectively retained in the graphite core of a GT-MHR at temperature >1000 °C and readily enters the helium coolant. The ^{110m}Ag isotope is the main concern. Releases of ^{110m}Ag during the 1600 °C heating test was unclear as the authors of Ref. [18] pointed out that its inventory was too small to be detected even if it was released during the test. Examination of the diffusivities of Ag in SiC and ZrC should indicate which layer retains ^{110m}Ag better. The effective diffusivity in ZrC at 1600 °C is ~1.5 × 10⁻¹⁶ m²/s (Figs. 7–5 in Ref. [22]), while it is about the same in SiC with UO₂ kernel (Fig. 10 in Ref. [23]). (Note that these diffusivities are inferred from post-irradiation heating experiments.) ZrC probably holds silver no better than SiC does, offering no benefit or disadvantage.

Bullock [23] reported results from a post-irradiation annealing study of different types of particle–fuel designs on fission product release. At 1200 °C, 1350 °C and 1500 °C, the only fuel particle type that fully retained all monitored fission products (Cs, Ag, Eu and

Ce) was the one having 9.1 ± 1.8 μm ZrC overcoat on the UO₂ kernel. The annealing time was over 12,000 h. The other types of particle designs were conventional TRISO-coated UO₂ kernel, UC₂ kernel, a mixture of UO₂ and UC₂ kernel, and a UO₂ kernel having ZrC dispersed in the buffer layer.

7.2. Disadvantages

7.2.1. Lack of data on high-burnup long-duration irradiations

To date, there is no experimental data on high-burnup, long-duration irradiation test of the ZrC-coated TRISO. The longest achieved only 4.5% FIMA for 100 EFPD [17]. Severely limited data necessitates extrapolation of low-burnup, low-duration irradiations to ultra-high burnup, long-duration irradiation conditions anticipated in the reactor. However, first-principles thermodynamic arguments support the performance of ZrC.

7.2.2. Lower strength

Due to the lack of reliable data in the literature, the characteristic strength of ZrC listed in Table 2 was assumed to be 70%, 50%, 30% and 10% that of the SiC. For comparison purposes, for a high density, CVD-deposited β-SiC, Ref. [24] reported a fracture stress measured in bending of about 1000 MPa from room temperature to ~900 °C, increasing to 1300 MPa at 1400 °C. On the other hand, Ref. [25] indicated that from fluence of 1.9 × 10²⁵–4.2 × 10²⁵ n/m² and from 1020 °C to 1280 °C, the mean fracture stress of tubular SiC “TRISO surrogate” specimens determined by the internal pressurization test remained at about 337 MPa. Ref. [26] reported the ultimate bend strength of ZrC to be ~125 MPa at 1000 °C and 150–160 MPa at 1600 °C. These pieces of data imply that ZrC is not as strong as SiC. If the strengths of the two materials were to be directly compared using only these data, for the worst-case scenario, the strength of ZrC appears to be only about 10–12% of the SiC strength. The lack of data necessitates an assumption of several ZrC strength values, starting from 10% of the SiC strength.

The Weibull modulus of ZrC was reported in Ref. [26] to be 6–9. A value of 6 was used. A value of 7 or 8 could have been used, but all the calculations were performed and finished using the Weibull modulus of 6 before Ref. [26] was studied.

7.2.3. More easily oxidized

Because ZrC readily reacts with oxygen at elevated temperatures (its important role as an oxygen getter; this aspect will be discussed in more detail later), were air or water vapor to come into contact with fuel compacts during an accident, the ZrC load-bearing layer would quickly oxidize and lose containment. An OPyC is assumed to have cracked, been consumed by reaction with air or water, or otherwise become permeable.

Since it is not advisable to substitute ZrC for SiC without having an oxygen getter on the kernel to prevent CO from oxidizing the ZrC, the performance of this particular TRISO design was not evaluated.

Cracks in the IPyC have always been observed in irradiated fuel particles, thus providing easy pathways for CO to interact with ZrC.

7.2.4. Higher resonance neutron absorption

Zirconium behaves like a non-burnable poison due to resonance neutron absorption, which will reduce neutron absorption in Pu. For a comparison purpose, there are 2.25 times more absorption in Zr compared to Si, resulting in a 1% decrease in uranium absorptions for a UO₂ kernel [27].

7.2.5. Larger thermal expansion coefficient

ZrC exhibits ~20–30% higher thermal expansion coefficient than SiC [9,11,12], resulting in a larger thermal strain. Both the inner and outer pyrolytic carbon layers will experience additional stresses.

7.2.6. Fabrication of CVD ZrC

The main hurdle in applying the ZrC layer is the difficulties in controlling zirconium halide entering the coating chamber [28]. However, based on past ZrC process development experience, a bromide process developed at JAERI [22,29] and a ZrCl₄ sublimation process developed at LANL proved to be the most reliable with respect to controlling Zr-halide supply to the coater [30,31]. Although these processes have been demonstrated only in laboratory-scale coaters and although studies will need to be performed to reliably supply Zr-halide to industrial-size coaters, the techniques appear very promising. Both studies concluded that [30]: (1) practical coating rates for ZrC were ~0.2–0.5 μm/min, which was about that of SiC and (2) the 1500 °C optimum coating temperature was approximately the optimum coating temperature for SiC.

The Commissariat 'a l'Energie Atomique (CEA) and Areva has been working on the laboratory-scale ZrCl₄ deposition process with C₃H₆ gas, as part of the "ANTARES" (Areva New Technology for Advanced Reactor Energy Supply) program aimed to conduct a research and development to produce high quality VHTR fuel [32]. Preliminary tests achieved a ~35-μm thick ZrC layer with the majority of the layer (30 μm) composing of almost stoichiometric ZrC with a maximum chlorine content of 0.2 at%. Development works are being done at CEA Grenoble to optimize the ZrC layer deposition parameters.

7.2.7. No QA technique developed yet

As pointed out by the unknown reviewer, "a key disadvantage with respect to ZrC is that the current QA technique to measure SiC defects – the burn leach test – will not work on ZrC TRISO. There is no accepted alternative method yet developed."

8. Evaluating ZrC getter on kernel with conventional TRISO

ZrC is known to readily react with CO gas. The particle fuel can benefit from this characteristic by applying a ZrC getter over a PyC seal on the kernel. The seal coat is required to protect the kernel from gases used to deposit ZrC.

8.1. Advantages

8.1.1. Elimination of CO pressure

Above 1000 °C, ZrC scavenges CO via the reaction:



The relevant reaction between ZrC and molecular oxygen is



and the oxygen partial pressure of the above reaction can be expressed as

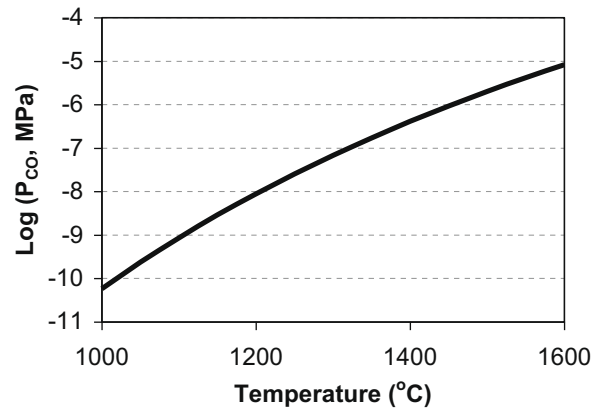


Fig. 2. Predicted CO pressure in the presence of the ZrC getter.

$$RT \ln(0.1p_{\text{O}_2}) = -8.981 \times 10^5 + 175.35(T + 273) \quad (\text{Ref. 4}). \quad (6)$$

The unit of pressure is in MPa and the unit of temperature is in °C.

The CO formation reaction is



and the oxygen partial pressure of the above reaction can be expressed as

$$RT \ln(0.1p_{\text{O}_2}) = RT \ln(0.1p_{\text{CO}})^2 - 1.138 \times 10^5 - 87.209 \times (T + 273) \quad (\text{Ref. 4}). \quad (8)$$

The unit of pressure is in MPa and the unit of temperature is in °C.

Thermodynamic equilibrium requires that the oxygen partial pressures of the two systems expressed by Eqs. (6) and (8) be equal. Equating the two at a fixed temperature determines the CO pressure. Fig. 2 plots the equilibrium CO pressure in the presence of the ZrC getter. ZrC is predicted to suppress the CO pressure well below 0.1 MPa under all conditions.

Proksch et al. [15] studied efficiencies of different oxygen scavengers present in the UO₂ kernel. Batches of low-density UO₂ kernels with 5 mol % of ZrC, TRISO-coated, were irradiated up to 1450 °C for 175 days, reaching a burnup of 6.2% FIMA. The post-irradiation CO release measurement was performed at 1500–1600 °C. It was found that the reduction in CO release was about 35–45%. It is important to realize that the experiment had only 5 mol % of ZrC inside the kernel. Having a solid ZrC layer surrounding the kernel would undoubtedly be much more effective.

8.1.2. Elimination of kernel migration

The presence of CO gas is one of the necessary conditions for kernel migration, which can contribute to fuel failure. Kernel migration, sometimes referred to as an amoeba effect, takes place when the kernel physically moves up the temperature gradient. The mechanism is the following: the thermodynamics of the reaction: $2\text{CO} \rightleftharpoons \text{CO}_2 + \text{C}$ favors the left side at high temperature. Carbon removal (and CO formation) occurs on the hot side while carbon deposition occurs at the cold side. The end result is a net transport of carbon from the high temperature region to the low temperature region, pushing the kernel to the hot side. If there is no temperature gradient across the fuel particle or if the gradient is very low (<10⁴ K/m), such as in German fuel spheres, the migration cannot take place. Low fuel temperature and suppression of CO also inhibit the phenomenon. For example, a UCO (uranium oxycarbide) kernel with the right stoichiometry of uranium and carbon can take up all the excess oxygen, and the phenomenon

cannot take place. Kernel migration is discussed in greater details in Refs. [33–36,44] and on pp. 2–33 to 2–43 in Ref. [37]. Having ZrC on the kernel to getter CO would undoubtedly prevent the amoeba effect.

8.1.3. Elimination of CO–SiC reaction

CO is known to react with SiC to form SiO gas [4] (if the IPyC becomes permeable or is cracked). Thus, the getter eliminates this undesirable reaction.

8.2. Disadvantages

8.2.1. Lack of data on high-burnup long-duration irradiation test

To date, there has been no experimental data reported on high-burnup, long-duration irradiation tests of the ZrC getter. Proksch et al.'s experiment [15] came the closest to studying the performance of the ZrC scavenger, but, unfortunately, the ZrC was embedded in the kernel instead of surrounding it. The lack of data necessitates the use of first-principles thermodynamic arguments to justify the performance of the ZrC getter.

8.2.2. Higher resonance neutron absorption

As discussed earlier, Zr behaves like a non-burnable poison and will reduce neutron absorption in Pu.

8.2.3. Fabrication becomes slightly more complex

Additional layers of the PyC seal coat and the ZrC getter would make the fabrication slightly more complex and would increase the fabrication cost.

8.2.4. Potential of greater fission-product loss from the kernel

The ZrC getter effectively lowers the oxygen potential of the kernel. In doing so, it reduces all fission product oxides exhibiting standard-state Gibbs formation energies higher than that of ZrO_2 . This inadvertently results in increasing the metallic fission product inventory in the kernel. Although some metals may diffuse out of the kernel, they are probably stopped by the ZrC layer. More research on this topic is needed. Nonetheless, a good aspect of reducing fission product oxides to metals is the reduction of kernel swelling by solid fission products because the atomic volumes of metallic elements are smaller than those of their oxides.

Performance of SiC-coated TRISO fuel having the ZrC oxygen scavenger was assessed. The CO pressure was assumed to be zero all the time. During the postulated EOL accident, failure of the SiC coating was predicted to be $10^{-3.59}$. The getter helped lower the failure probability, but the failure was still high due to SiC-fission product interaction.

9. Evaluating the ZrC getter on kernels with ZrC-coated TRISO

Performance of ZrC-coated TRISO fuel having the ZrC oxygen scavenger was evaluated. The CO pressure was assumed to be zero all the time. During the postulated EOL accident, for the case of ZrC having 10% of the characteristic strength of SiC, ZrC failure was predicted to be $10^{-4.26}$. Although ZrC was assumed to have only 10% of the SiC strength, it still performed better than SiC because of the absence of ZrC corrosion by fission products.

10. Evaluating an alloy IPyC with normal TRISO

10.1. Advantage

An intact IPyC layer is essential for the SiC (or ZrC) interlayer to successfully contain fission products. If the IPyC breaks, it will pull away tangentially at that location because of the irradiation-in-

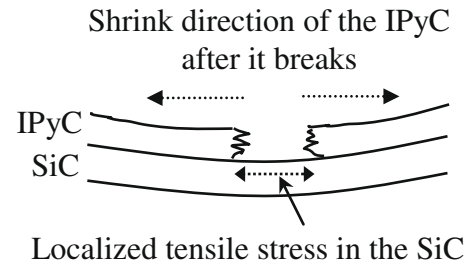


Fig. 3. Effect of a broken IPyC on SiC.

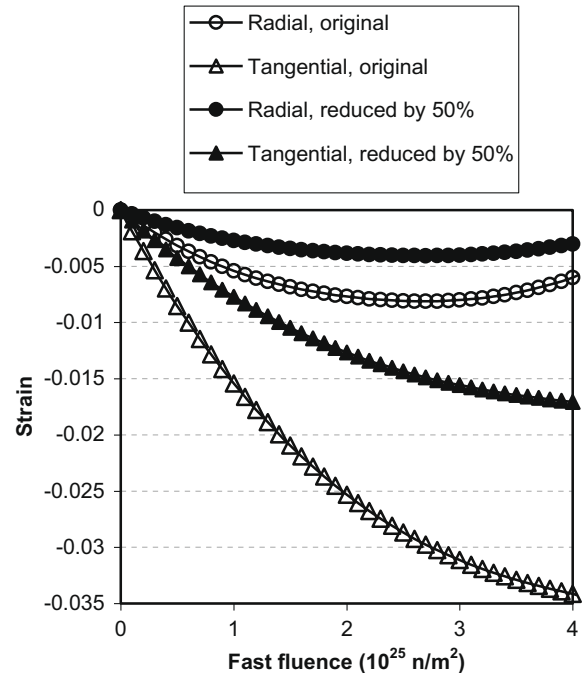


Fig. 4. Irradiation-induced dimensional changes of the PyC–SiC alloy.

duced shrinkage. This creates a localized, intensified tensile stress in the SiC underneath, making it susceptible to breaking. Fig. 3 depicts the effect of a broken IPyC on SiC.

Kaae et al. [38] studied the dimensional change of PyC co-deposited with 33 wt.% of SiC. He found that the tangential shrinkage of the alloy IPyC was reduced by at least 50%. When the IPyC shrinks less, it experiences a smaller tangential stress and the stress-induced failure is lower. One of the design features of the Deep Burn fuel is co-deposition of the IPyC with 33 wt.% of SiC to reduce the tangential shrinkage by $\sim 50\%$.

Fig. 4 presents the modified irradiation-induced strains of pyrocarbon materials. The original curves were obtained from General Atomics (Ref. [8]). The shrinkage is categorized into two directions – the tangential direction, which is parallel to the SiC (or ZrC) layer, and the radial direction.

10.2. Disadvantage

Since the IPyC shrinks at a lesser extent, it holds the SiC (or ZrC) in compression less effectively. Thus, the load-bearing interlayer experiences higher tangential stresses.

Performance of normal TRISO with the alloy IPyC was assessed. Since the CO pressure during the postulated EOL accident could not be estimated with high accuracy, values of 60 MPa and 100 MPa were assumed. During the accident, the SiC failure was predicted to be

- $10^{-2.03}$ for the case with 100 MPa of CO pressure,
- $10^{-2.99}$ for the case with 60 MPa of CO pressure.

These very high failures were due to the very large CO pressure. Compared to the normal TRISO with no IPyC alloy, the current case exhibited a slightly higher failure, corresponding to the understanding that the alloy IPyC holds the SiC in compression less effectively.

11. Evaluating the alloy IPyC with ZrC-coated TRISO

Similar to the case of ZrC-coated TRISO with no IPyC alloy and with no oxygen getter, this was deemed to be a poor design and was not evaluated.

12. Evaluating the alloy IPyC with conventional TRISO having ZrC getter

Performance of normal TRISO having the alloy IPyC and the ZrC getter was assessed. The CO pressure was assumed to be zero all the time. During the postulated EOL accident, the SiC failure was predicted to be $10^{-3.59}$. This rather high failure was due to the SiC-fission product interaction.

13. Evaluating the alloy IPyC with ZrC-coated TRISO and a ZrC getter

Performance evaluation of ZrC-coated TRISO fuel with the alloy IPyC and the ZrC getter was carried out. The CO pressure was assumed to be zero all the time. During the postulated EOL accident, for the case of ZrC having 10% of the characteristic strength of SiC, the failure of ZrC was predicted to be $10^{-4.26}$. Although ZrC was assumed to have only 10% of the SiC strength, it still performed better than the SiC-coated particle fuel of the same design (see previous section) because there was no ZrC-fission product corrosion.

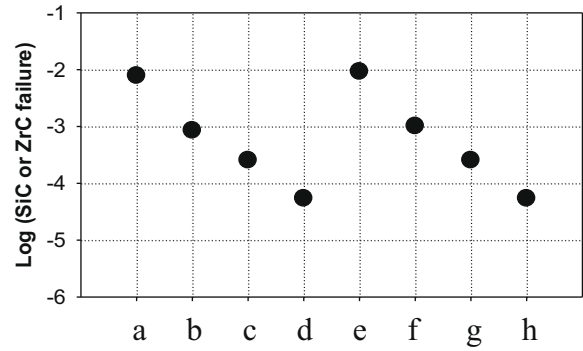
Fig. 5 summarizes the performance of different particle–fuel design features.

The ZrC-coated TRISO with the ZrC getter with or without the alloy IPyC is predicted to perform the best. Although it may not be clear from Fig. 5 what the benefit of alloying the IPyC is, as discussed earlier, having the IPyC in less tension reduces crack-propagation in the ZrC coating. This phenomenon was not modeled in PISA so the effect cannot be seen in the plot. Had the effect been modeled into PISA, the data points for the cases with no alloy IPyC would have shifted upward. Thus, it can be concluded that the ZrC-coated TRISO with the getter and with the alloy IPyC represents the best particle–fuel design for Deep Burn. The remaining analysis was performed on this design.

For each of four ZrC characteristic strengths listed in Table 2, the kernel diameter was varied from 200 to 350 μm , and the buffer thickness was varied from 60 to 140 μm . All other coating layer thicknesses remained fixed. The objective was to select combinations of kernel diameters and buffer thicknesses that resulted in ZrC interlayer failure $<10^{-4}$. Obviously, one combination that already satisfied this requirement was the 200- μm kernel with a 100- μm buffer.

14. Results

Fig. 6 illustrates the tangential stresses in the IPyC, ZrC, and OPyC predicted by PISA. To simplify the interpretation of the plot, three kernel sizes are shown (200, 250 and 300 μm) with a single 100- μm buffer thickness. The tangential stress in the IPyC increased at the beginning because of the fast-neutron-induced shrinkage in the tangential direction. It leveled off and reduced



where:

a = normal TRISO, no getter, no IPyC alloy,
 $P_{\text{CO}} = 100 \text{ MPa}$

b = normal TRISO, no getter, no IPyC alloy,
 $P_{\text{CO}} = 60 \text{ MPa}$

c = normal TRISO, with getter, no IPyC alloy

d = ZrC-coated TRISO, with getter, no IPyC alloy

e = normal TRISO, no getter, with IPyC alloy,
 $P_{\text{CO}} = 100 \text{ MPa}$

f = normal TRISO, no getter, with IPyC alloy,
 $P_{\text{CO}} = 60 \text{ MPa}$

g = normal TRISO, with getter, with IPyC alloy

h = ZrC-coated TRISO, with getter, with IPyC alloy

Fig. 5. Performance differences among various particle–fuel design features.

after a fluence of $\sim 0.5 \times 10^{25} \text{ n/m}^2$ because the irradiation-induced creep relaxation overcame the irradiation-induced dimensional change. The creep continued to relax the stress and the IPyC became almost stress-free at the EOL. Only one set of plots for the IPyC and OPyC is shown because the curves for all three kernel sizes are almost identical.

The shrinkage of the IPyC maintained a compressive tangential stress in the ZrC (owing to an assumed strong IPyC–ZrC interface). The initial rise of the compressive stress in the ZrC was directly due to the increasing shrinkage of the IPyC. As the IPyC became relaxed by creep and as the fission-gas pressure built up with fluence, the tangential tensile stress in the ZrC increased. Among the three curves shown, the ZrC associated with a 300- μm kernel experienced the largest stress because fission-gas pressure was highest. For this kernel size, the accident condition at the EOL drove the ZrC stress up to 75 MPa, as the fission-gas pressure rose by 47%. For the extreme case of a 350- μm kernel with a 60- μm buffer (not shown in the plot), PISA predicted the ZrC stress during the postulated accident to reach 720 MPa.

Figs. 7–10 display maximum failure probabilities of the ZrC load-bearing layer having 70%, 50%, 30% and 10% of the characteristic strength of SiC, respectively. The maximum failure probability always occurred during the postulated accident, as this was the peak of the internal gas pressure.

The trends observed in Figs. 7–10 are:

1. For the same buffer thickness and ZrC strength, bigger kernels generated more fission gas, thus, ZrC failure was higher than the case with smaller kernels.

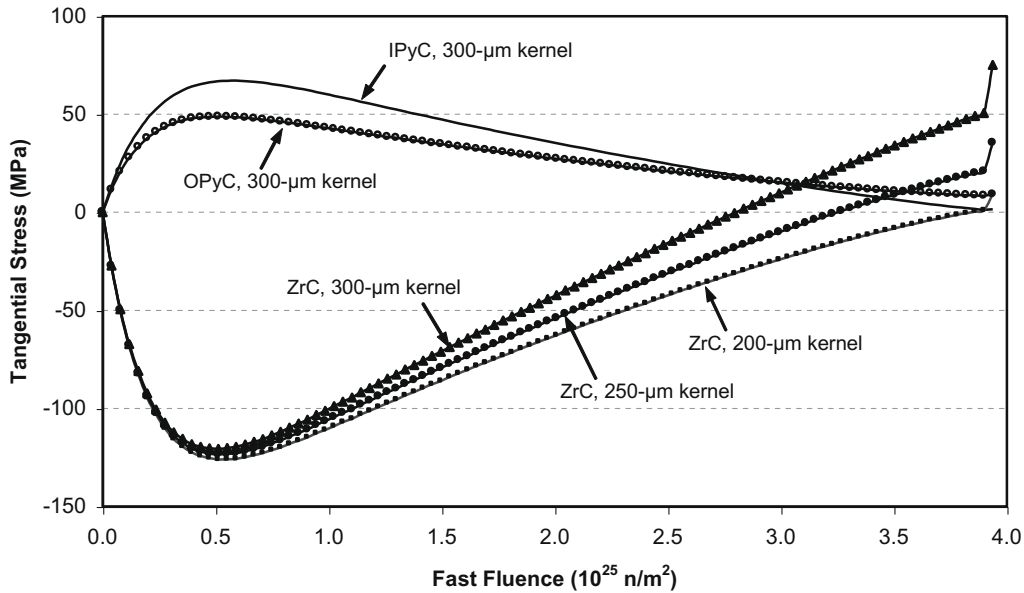


Fig. 6. Tangential stresses in IPyC, ZrC and OPyC predicted by PISA. Only cases with 100-μm buffer thickness are shown.

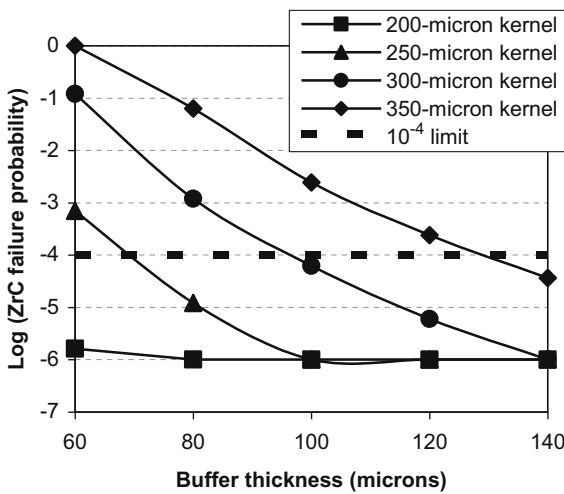


Fig. 7. Failure probabilities of ZrC having 70% of the characteristic strength of SiC.

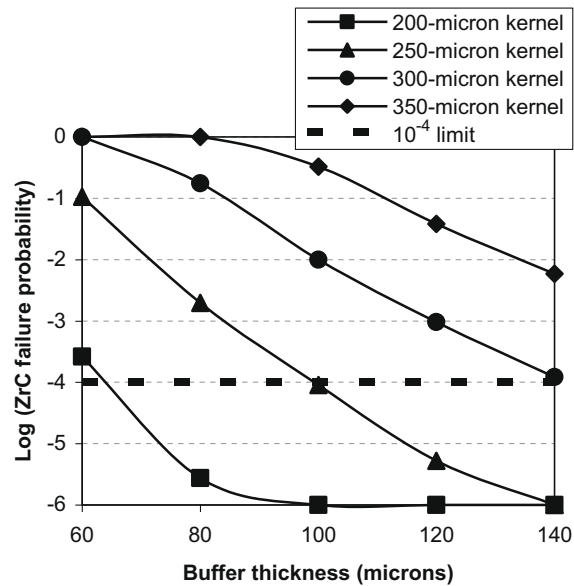


Fig. 9. Failure probabilities of ZrC having 30% of the characteristic strength of SiC.

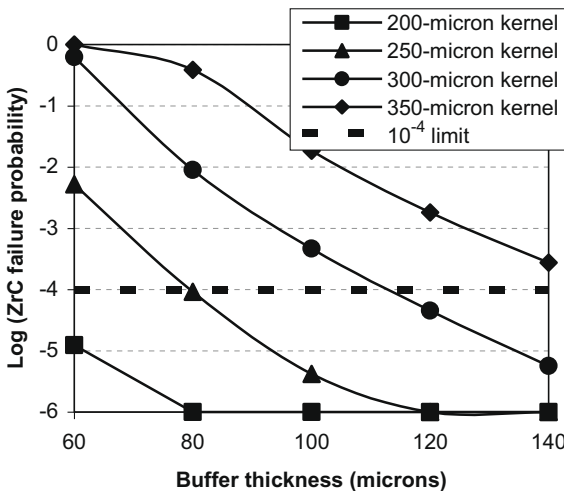


Fig. 8. Failure probabilities of ZrC having 50% of the characteristic strength of SiC.

2. For the same kernel size and ZrC strength, larger buffer thicknesses resulted in a reduced gas pressure, thus, ZrC failure decreased with increasing buffer size.
3. As the characteristic strength of ZrC decreased, the ZrC experienced higher failure for the same kernel size and buffer thickness (unless the failure probability was already at 100% or at 10^{-6}).

Any data point below the 10^{-4} limit represented an acceptable combination of kernel diameter and buffer thickness. For instance, for the case of ZrC having 70% of the characteristic strength of SiC (Fig. 7), the 200-μm kernel can have any buffer size in the range studied, while the 250-μm kernel needed at least ~70 μm of buffer thickness. To be most conservative, prediction of failures was based on the lowest ZrC characteristic strength (Fig. 10). Thus, the only choice for Deep Burn particle fuel appears to be a 200-μm kernel coupled with at least a 100-μm thick buffer.

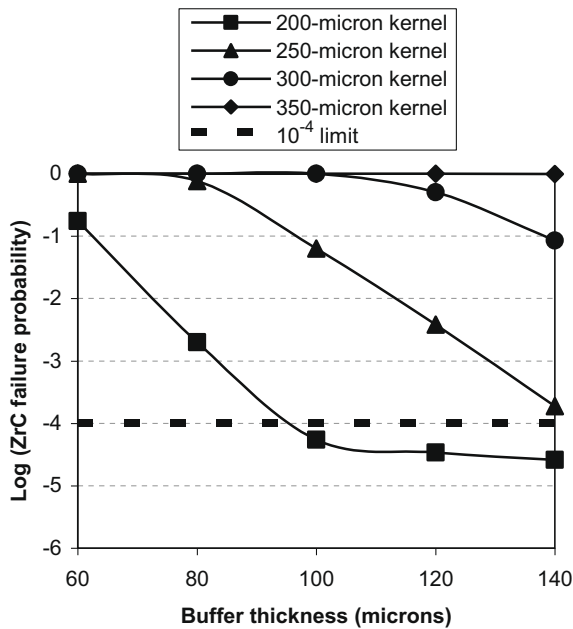


Fig. 10. Failure probabilities of ZrC having 10% of the characteristic strength of SiC.

Care must be taken to make certain that the kernel–coating–mechanical interaction does not occur, as this would lead to rapid fuel failure as analyzed by Martin [37]. Taking the volumetric kernel swelling due to solid fission products to be 1% per % FIMA, at 70% FIMA, the radius of the 200- μm kernel would have swollen by 70 μm . The volume of the condensed buffer is assumed to occupy $\frac{1}{2}$ of its initial volume. The thickness of the PyC seal coat and the ZrC getter are assumed not to change with burnup. Fig. 11 shows the result of a calculation of the free space between the condensed buffer and the IPyC as a function of initial buffer thickness.

Enough free space at ultra-high burnup to avoid a hard mechanical contact between the condensed buffer and the IPyC must be made available. Unfortunately, with no irradiation data on ultra-high burnup TRISO fuel, conclusions cannot be drawn on how much the initial buffer thickness would be needed but a minimum clearance of $\sim 15\text{--}20\ \mu\text{m}$ at 70% FIMA should be provided. Based on Fig. 11, the required minimum initial buffer thickness is approximately 150 μm . It is also important to realize that the highest solid fission product swelling coefficient of 1% per % FIMA was used. Perhaps, if the actual value turns out to be, for instance, 0.5% per % FIMA, additional 35 μm of free space is regained, and the buffer thickness of 100 μm suffices.

Hence, the only choice for Deep Burn particle fuel is a 200- μm kernel coupled with at least 150- μm buffer. This design satisfies the 10^{-4} limit with a reasonably wide margin (see Fig. 10 and extrapolate the buffer thickness to 150 μm). In reality, ZrC most likely has more than 10% of SiC strength, and the failure will be lower than analyzed here.

Although it would be desirable for PISA to incorporate the effect of hard mechanical contact between the condensed buffer layer and the IPyC to further study the performance of the fuel particle, the fuel should never operate in this region (even though the fuel may be predicted to survive). Preventative measures such as a large buffer must be provided to avoid the contact. Then, the assumption built into PISA of uncoupling the kernel, the PyC seal coat, the ZrC getter and the buffer from the rest of the layers is valid.

After some burnup, swollen kernel would undoubtedly exert excessive stresses on the PyC seal coat and the ZrC getter, and the two layers would eventually break. The kernel would be

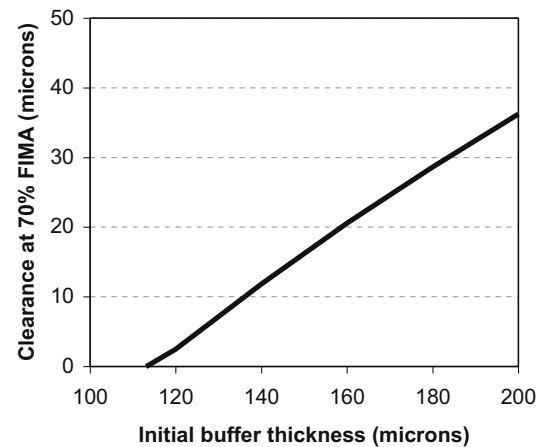


Fig. 11. Clearance between condensed buffer and IPyC at 70% FIMA as a function of initial buffer thickness. The BOL kernel diameter is 200 μm .

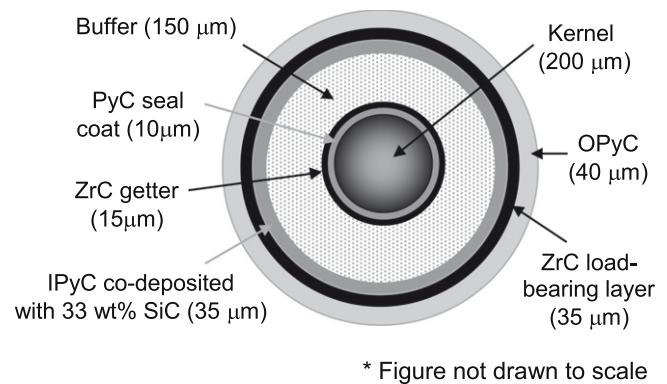


Fig. 12. Proposed particle–fuel design.

extruded through the crack and release some CO into the buffer layer. The probability that the CO gas would come into contact with the ZrC load-bearing layer possibly through cracks in the alloy IPyC (which is more crack-resistant than conventional IPyC with no SiC alloy) would be very low compared to it reacting directly with the outer surface of the ZrC getter. Therefore, cracking of the ZrC getter should not be of concern with respect to its ability to continue eliminating CO.

15. Future work

To obtain a more complete picture of the reactor core design, a depletion analysis is required to determine the fuel packing fraction⁸ that yields the highest burnup. Besides the initial buffer thickness, the fuel-to-moderator ratio is another adjustable parameter that places a limit on the packing fraction.

The concept of kernel dilution,⁹ when the fuel constituents are diluted in a neutronically-inert matrix such as yttria stabilized zirconia [39–42] or dispersed in a carbon matrix to form a porous spherical kernel [43], deserves consideration. The main benefit of diluting the kernel is to reduce neutron self-shielding, thereby increasing burnup and the cycle length. Fission gas generation in

⁸ The fuel packing fraction is the ratio of the total particle fuel volume to the fuel compact volume.

⁹ This concept is conventionally termed “inert matrix fuel.” The Journal of Nuclear Materials vol. 274, issues 1–2, pp. 1–227, published in August 1999 contains many articles on this subject.

each particle fuel will be lower as well, reducing the ZrC failure even more. However, there are fabrication issues with the carbon matrix fuel. Furthermore, the fuel packing fraction would need to be increased to obtain the same fissile loading. This might introduce an additional risk of coating failure during fuel compact fabrication.

Finally, high-burnup, long-duration irradiation tests and post-irradiation heating tests of particle fuel of this design or of similar designs need to be conducted before fuel performance evaluations can be accepted and used for fuel design.

16. Conclusions

The performance of ZrC was justified based on first-principles thermodynamic arguments and on extrapolation of low-burnup, low-duration irradiations to ultra-high burnup, long-duration irradiation conditions anticipated in the reactor. ZrC appears to be the material of choice to eliminate CO and to be a pressure vessel to allow the particle fuel to operate to a very high temperature in excess of 2000 °C without integrity degradation due to fission product attack and thermal decomposition. This modeling work provides grounds for future high-burnup, long-duration irradiation tests and Deep Burn fuel development.

The ZrC-coated fuel design recommended for Deep Burn has a 200- μm kernel diameter coupled with at least 150- μm buffer thickness, together with the ZrC getter on the PyC seal coat over the kernel and the alloy IPyC. PISA predicted the failure probability of this particle design to be $<10^{-4}$ under all conditions. The following is a proposed fabrication route for the Deep Burn particle fuel:

1. Fabricate a 200- μm kernel with oxygen-to-metal ratio <2 .
2. Coat the kernel with a 10- μm PyC seal.
3. Apply a 15- μm ZrC oxygen getter layer.
4. Deposit a minimum of 150- μm buffer.
5. Co-deposit a 35- μm highly-isotropic IPyC with 33 wt.% SiC.
6. Coat with a 35- μm ZrC load-bearing layer.
7. Finish the particle with a 40- μm OPyC layer.

Fig. 12 depicts the proposed particle–fuel design.

Acknowledgement

The author is very thankful to the following individuals (alphabetically):

- Dr. Donald McEachern at General Atomics for his time to review this paper and for his generous advice on all issues related to particle fuel design and GT-MHR technology.
- Professor Donald Olander at the University of California at Berkeley for his time to review this paper and for his generous advice on various issues.
- Dr. Francesco Venneri at General Atomics for his generous advice on various issues and for the funding of the project.
- The US taxpayers whose tax money is the ultimate source of the funding of this project.
- The unknown reviewer who pointed out several errors in the manuscript and who directed the author to a paper pertaining to the attainment of high burnup HTR fuel.

This work was supported by a DOE Deep Burn grant.

References

- [1] F. Venneri et al., Deep Burn transmutation: a practical approach to the destruction of nuclear waste in the context of nuclear power sustainability, General Atomics, FDO-E00-N-TRT-X-000132, December, 2001.
- [2] D.R. Olander, University of California at Berkeley, private communication.
- [3] D.D. Lanning, C.E. Beyer, C.L. Painter, FRAPCON-3: modifications to fuel rod material properties and performance models for high-burnup application, Pacific Northwest National Laboratory, NUREG/CR-6534, vol. 1, PNNL-11513, October, 1997.
- [4] T.B. Lindemer, Thermochemical analysis of gas-cooled reactor fuels containing Am and Pu Oxides, ORNL/TM-2002/133, September, 2002.
- [5] D. Pelessone, PISA: a one-dimensional spherically symmetric computer program to perform thermal and stress analysis of irradiated fuel particles, General Atomics, CEGA-M-92-2052, July, 1992.
- [6] R.C. Martin, Compilation of fuel performance and fission product transport models and database for MHTGR design, Oak Ridge National Laboratory, ORNL/NPR-91/6, October, 1993.
- [7] The CRP-6 Benchmark on HTGR fuel behavior under normal operation, nuclear fuels and structural materials for the next generation nuclear reactors, Reno, Nevada, June, 2006.
- [8] F. Ho, NP-MHTGR Material Models of Pyrocarbon and Pyrolytic Silicon Carbide, General Atomics, CEGA-002820, Review, 1, July, 1993.
- [9] <http://www.ceramics.nist.gov/srd/scd/Z00220.htm>.
- [10] A.G. Lanin, I.I. Deryavko, J. Eur. Ceram. Soc. 20 (2000) 209–213.
- [11] <http://www.ceramics.nist.gov/srd/scd/Z00251.htm>.
- [12] A.W. Weimer, Carbide, Nitride and Boride Material Synthesis and Processing, Springer, US, 1996 (December).
- [13] G. Miller, D. Petti, D. Varacalle Jr., J. Maki, J. Nucl. Mater. 317 (2003) 69–82.
- [14] T. Ogawa, K. Ikawa, High Temp. Sci. 22 (1986) 179–193.
- [15] E. Proksch, A. Strigl, H. Nabielek, J. Nucl. Mater. 139 (1986) 83–90.
- [16] T. Ogawa, K. Ikawa, K. Fukuda, S. Kashimura, K. Iwamoto, Nuclear Fuel Performance, BNES, London, 1985, p. 163.
- [17] K. Minato, T. Ogawa, K. Sawa, A. Ishikawa, T. Tomita, S. Iida, H. Sekino, Nucl. Technol. 130 (2000) 272–281.
- [18] K. Minato, T. Ogawa, K. Fukuda, H. Nabielek, H. Sekino, Y. Nozawa, I. Takahashi, J. Nucl. Mater. 224 (1995) 85–92.
- [19] K. Minato, T. Ogawa, K. Fukuda, H. Sekino, I. Kitagawa, N. Mita, J. Nucl. Mater. 249 (1997) 142–149.
- [20] T. Ogawa, K. Fukuda, S. Kashimura, T. Tobita, F. Kobayashi, S. Kado, H. Miyaniishi, I. Takahashi, T. Kikuchi, J. Am. Ceram. Soc. 75 (1992) 2985–2990.
- [21] http://gt-mhr.ga.com/safety_all.html.
- [22] Fuel performance and fission product behaviour in gas cooled reactors, International Atomic Energy Agency, IAEA-TECDOC-978, November, 1997.
- [23] R.E. Bullock, J. Nucl. Mater. 125 (1984) 304–319.
- [24] T. Gulden, J. Am. Ceram. Soc. 52 (1969) 585–590.
- [25] L.L. Snead, T. Nozawa, Y. Katoh, T. Byun, S. Kondo, D.A. Petti, J. Nucl. Mater. 371 (2007) 329–377.
- [26] A. Lanin, M. Fedotov, V. Glagolev, Strength and plasticity of zirconium carbide, translated, National Technical Information Service, Article no. AD727942, March, 1971.
- [27] C. Ellis, Effect of use of zirconium carbide coatings on the VHTR core nuclear design, General Atomics, PC-000514, December, 2003.
- [28] C.M. Hollabaugh, R.D. Reiswig, P. Wagner, L.A. Wahman, R.W. White, J. Nucl. Mater. 57 (1975) 325–332.
- [29] T. Ogawa, K. Ikawa, K. Iwamoto, J. Nucl. Mater. 97 (1981) 104–112.
- [30] Development Plan for Advanced High Temperature Coated Particle Fuels, General Atomics, PC-000513, January, 2004.
- [31] P. Wagner, L.A. Wahman, R.W. White, C.M. Hollabaugh, R.D. Reiswig, J. Nucl. Mater. 62 (1976) 221–228.
- [32] F. Charollais, S. Fonquernie, C. Perrais, M. Perez, O. Dugneq, F. Cellier, G. Harbonnier, M. Vitali, Nucl. Eng. Des. 236 (2006) 534–542.
- [33] F. Homan, T. Lindemer, E. Long, T. Tiegs, R. Beatty, Nucl. Technol. 35 (1977) 428–441.
- [34] Y. Choi, J.K. Lee, J. Nucl. Mater. 357 (2006) 213–220.
- [35] M. Wagner-Löffler, Nucl. Technol. 35 (1977) 392–402.
- [36] C.L. Smith, Nucl. Technol. 35 (1977) 403–412.
- [37] D.G. Martin, Nucl. Eng. Des. 35 (1977) 403–412.
- [38] J.L. Kaee, D.W. Stevens, J.C. Bokros, Carbon 10 (1972) 285–292.
- [39] Y.-W. Lee, H.S. Kim, S.H. Kim, C.Y. Joong, S.H. Na, G. Ledergerber, P. Heimgartner, M. Pouchon, M. Burghartz, J. Nucl. Mater. 274 (1999) 7–14.
- [40] C. Degueldre, Ch. Hellwig, J. Nucl. Mater. 320 (2003) 96–105.
- [41] H.J. Matzke, V.V. Rondinella, T. Wiss, J. Nucl. Mater. 274 (1999) 47–53.
- [42] C. Degueldre, J.M. Paratte, J. Nucl. Mater. 274 (1999) 1–6.
- [43] G.W. Horsley, R.A.U. Huddle, H. Bairiot, J. Van Geel, The manufacture of plutonium-fuelled fission-product-retaining coated particles for irradiation in the dragon reactor experiment, DRAGON Project Report 525, 1967.
- [44] Oya Özdere Güllü, Üner Çolak, Bora Yıldırım, J. Nucl. Mater. 374 (2008) 168–177.